

# R-SFLLM: Jamming Resilient Framework for Split Federated Learning with Large Language Models

Aladin Djuhera , *Graduate Student Member, IEEE*, Vlad C. Andrei , *Graduate Student Member, IEEE*,  
Xinyang Li , *Graduate Student Member, IEEE*, Ullrich J. Mönich , *Senior Member, IEEE*,  
Holger Boche , *Fellow, IEEE*, and Walid Saad , *Fellow, IEEE*

**Abstract**—Split federated learning (SFL) is a compute-efficient paradigm in distributed machine learning (ML), where components of large ML models are outsourced to remote servers. A significant challenge in SFL, particularly when deployed over wireless channels, is the susceptibility of transmitted model parameters to adversarial jamming that could jeopardize the learning process. This is particularly pronounced for word embedding parameters in large language models (LLMs), which are crucial for language understanding. In this paper, rigorous insights are provided into the influence of jamming LLM word embeddings in SFL by deriving an expression for the ML training loss divergence and showing that it is upper-bounded by the mean squared error (MSE). Based on this analysis, a physical layer framework is developed for resilient SFL with LLMs (R-SFLLM) over wireless networks. R-SFLLM leverages wireless sensing data to gather information on the jamming directions-of-arrival (DoAs) for the purpose of devising a novel, sensing-assisted anti-jamming strategy while jointly optimizing beamforming, user scheduling, and resource allocation. Extensive experiments using BERT and RoBERTa models demonstrate R-SFLLM’s effectiveness, achieving close-to-baseline performance across various natural language processing (NLP) tasks and datasets. The proposed methodology further introduces an adversarial training component, where controlled noise exposure significantly enhances the LLM’s resilience to perturbed parameters during training. The results show that more noise-sensitive models, such as RoBERTa, benefit from this feature, especially when resource allocation is unfair. It is also shown that worst-case jamming in particular translates into worst-case model outcomes, thereby necessitating the need for jamming-resilient SFL protocols.

**Index Terms**—6G, anti-jamming, large language model, resource allocation, split federated learning, wireless sensing

## I. INTRODUCTION AND MOTIVATION

Future 6G networks are anticipated to introduce a substantial leap toward highly integrated and intelligent connectivity at the edge, enabled by artificial intelligence (AI) [1] and machine learning (ML) [2]. However, in this envisioned hyper-connected and AI-assisted network, important questions and stringent requirements on resilience and trustworthiness arise,

both from a user and network perspective [3]. This imposes significant design challenges for emerging technologies, such as distributed and collaborative ML (DCML) [4], which may be targeted by adversarial attacks over the wireless medium. For instance, the distributed training of large language models (LLMs) faces unique challenges in ensuring data integrity and model robustness due to highly sensitive word embedding parameters. Much research has focused on addressing these challenges via adversarial AI training methods and model-based solutions [5], [6], and in [7], the authors closely investigated such attack and defense strategies in 6G networks, exposing critical vulnerabilities across all network layers. However, a number of important research questions remain underexplored, such as how these attacks can be orchestrated in practice, and how current and next-generation wireless network architectures, systems, and technologies can introduce proactive defense mechanisms, ideally by-design.

### A. Adversarial Poisoning in Wireless Federated LLM Training

Motivated by the increasing importance of end-user data privacy and associated privacy protection laws [8], DCML has been gradually shifting toward mechanisms such as federated learning (FL) [9] and split FL (SFL) [10]. These have proven to be privacy-preserving as only the respective model parameters, some parts of it or model gradients need to be exchanged. SFL in particular has emerged as a compute-efficient federated protocol, suitable for distributed training of large ML model architectures. Unlike traditional FL, in which the entire model is trained on each client, SFL splits the model, allowing for more compute-intensive parts to be outsourced to a remote server. This approach is particularly advantageous for LLM architectures that cannot be entirely processed at resource-constrained edge devices due to computational and memory limitations [11]. However, the practical realization of (S)FL over wireless networks faces challenges from the inherently unreliable wireless medium, limited bandwidth, and suboptimal resource allocation [12]. In addition, malicious actors such as jammers could target privacy and security aspects of (S)FL systems by intentionally poisoning data and models through adversarial noise. The particular importance of studying adversarial jamming attacks in SFL with LLMs is motivated by recent results from natural language processing (NLP) research [13], [14]. The authors in [13] study the susceptibility of LLMs to word embedding poisoning caused by noisy perturbations and show that by altering even a single word embedding vector, an adversary can subtly manipulate a

The authors were supported in part by the German Federal Ministry of Education and Research (BMBF) in the program “Souverän. Digital. Vernetzt.” within the research hub 6G-life under Grant 16KISK002, and also by the Bavarian Ministry of Economic Affairs, Regional Development and Energy within the project 6G Future Lab Bavaria. U. Mönich and H. Boche were also supported by the BMBF within the project “Post Shannon Communication - NewCom” under Grant 16KIS1003K. W. Saad was supported by the Center for Assured and Resilient Navigation in Advanced Transportation Systems (CARNATIONS) under the US Department of Transportation (USDOT)’s University Transportation Center (UTC) program under Grant 69A3552348324.

model to react abnormally to specific trigger words. Moreover, the severity of word embedding poisoning attacks for federated networks was studied in [14], showing that even a small number of compromised clients is sufficient to effectively deteriorate the global model. In federated systems over wireless networks, adversarial jamming emerges as a realistic threat for orchestrating such poisoning attacks by corrupting sensitive word embeddings during transmission. This covert adversarial perspective is in contrast to prior works on jamming in FL [15], [16], which do not consider the implications of poisoning the model’s reasoning capabilities. This is particularly critical in SFL, where word embeddings might be directly transmitted as intermediate split parameters. However, the detrimental impact of such attacks in SFL remains underexplored.

### B. Proactive and Resilient-by-Design Anti-Jamming in SFL

To preemptively safeguard LLM parameter transmissions in SFL against adversarial jamming attacks, proactive and in particular *resilient-by-design* approaches are needed [17]. This requires a simultaneous co-design of AI, resilience, beamforming, user scheduling, and resource allocation, thereby integrating resilience from a bottom-up approach, by design. In addition, such proactive defense mechanisms need to be agnostic of the respective jamming capabilities, including physical and spatial features. This is not the case for some more recent works, which tend to impose strong assumptions on the adversary’s knowledge and setup. For instance, [18] and [19] only consider single- or few-antenna jammers with common secrets being exchanged between legitimate parties. This essentially excludes so-called *worst-case* jammers with extensive system knowledge and capabilities [20], [21]. In order to develop universally applicable defense strategies for a wide range of jamming scenarios in SFL, system performance needs to be guaranteed for the worst-case. Thus, we need to generalize toward intelligent and reconfigurable worst-case jammers. In our prior work in [22], we motivated the study of how sensing-assisted network information can be harnessed to enhance existing mitigation schemes without the need for otherwise precise jamming statistics. Therein, we have shown that information on the jamming signal directions-of-arrival (DoAs) can be used to devise MIMO-OFDM anti-jamming strategies with exceptional performance. However, we did not discuss whether such sensing-assisted defense strategies can be straightforwardly applied to enhance the resilience in SFL over wireless networks. In particular, the impact of worst-case jamming needs to be quantified in order to study its influence on LLM model poisoning as compared to conventional jammers. In the subsequent sections, we provide thorough insights on these aspects, including an analysis on the minimum system rate that guarantees a reliable and resilient SFL training.

### C. Contributions

The main contribution of this paper is an analysis and framework for resilient SFL over wireless networks that will help close the gap between adversarial jamming attacks in SFL and LLM model poisoning. We provide insights into how jamming LLM word embeddings affects the global model

training and how the latter can be efficiently safeguarded by MIMO signal processing at the availability of sensing-assisted information. In summary, our key contributions include:

- We derive an analytical expression for the ML training loss divergence based on a relaxed  $(L_0, L_1)$ -smoothness assumption for LLM transformer architectures in the case of corrupted word embeddings. We show that its upper bound depends on the communication mean squared error (MSE), thereby motivating a wireless approach to resilience in SFL.
- We provide a novel analysis on the minimum system rate which guarantees a robust and reliable SFL training over the wireless network, thereby characterizing minimum network conditions based on the outage rate caused by the jammer.
- We develop R-SFLLM, a novel, sensing-assisted anti-jamming framework for resilient SFL with LLMs, which leverages the jamming signal’s DoAs to devise an anti-jamming strategy formulated as a joint optimization problem for beamforming, user scheduling, and resource allocation while maximizing the sum rate of the SFL participants. In this problem, any explicit knowledge about the jamming statistics is replaced by a surrogate expression that depends only on the jamming DoAs. We provide an efficient solution to the problem using an iterative water-filling approach [23].
- In order to benchmark R-SFLLM against worst-case conditions in SFL, we utilize the worst-case jamming strategy in our prior work [22], which minimizes the sum rate instead.
- We provide extensive simulations for BERT and RoBERTa models on various datasets, demonstrating near-optimal performance when anti-jamming is enabled and significantly worse outcomes for unprotected scenarios. We show that R-SFLLM introduces an additional adversarial training component as word embeddings are exposed to controlled noise since jamming cannot be mitigated perfectly. This exposure further helps improve the model robustness by teaching it to learn effectively even in the presence of interference [24].

The rest of this paper is organized as follows. Section II presents the R-SFLLM system model and derives expressions for the ML loss divergence and the minimum system rate. In Section III, we present the anti-jamming framework and develop the worst-case jamming strategy. Section IV discusses the simulation results and Section V concludes the paper.

## II. SYSTEM MODEL AND ADVERSARIAL ANALYSIS

### A. Wireless R-SFLLM System Model

We consider an SFL setup in which a set  $Q$  of  $Q$  legitimate clients cooperatively train transformer-based LLMs, which consist of embedding, attention and head layers. A natural choice in SFL with LLMs is to partition the model according to these blocks, assigning the embedding layer to the client and the compute-intensive attention and head layers to the server as outlined in Figure 1. This particular partitioning alleviates the computational load at the client while ensuring that word embeddings are processed close to the raw data, thereby enhancing privacy. Further partitioning the embedding block and transmitting intermediate layers instead increases the risk of sensitive information being exposed to adversarial attacks, such as model inversion [25]. During training, each

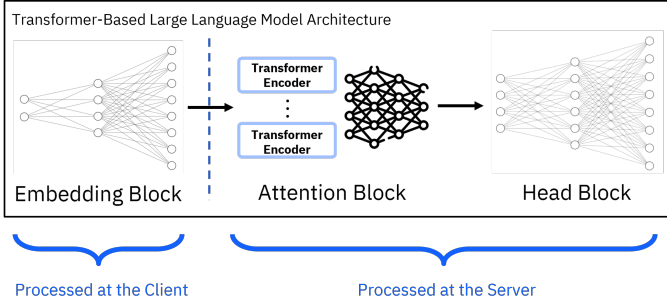


Fig. 1: SFL model split with LLM word embeddings being processed at the client and with attention and head layers being processed at the server.

user  $q \in \mathcal{Q}$  first computes the word embeddings  $e_q \in \mathbb{R}^E$  for its private data points and then maps the embeddings onto uncorrelated zero-mean, unit variance Gaussian symbols, which are then beamformed, power-scaled, and transmitted over the wireless channel to a dedicated server slice for further processing. To this end, we consider a MIMO-OFDM multiple access channel (MAC) in the uplink. Each user  $q$  is equipped with  $N_{T_q}$  antennas and transmits the signal  $\mathbf{x}_{qnk}$ , which is a composite of the binary user scheduling  $\alpha_{qnk}$ , transmit power  $p_{qnk}$ , beamforming vector  $\mathbf{w}_{qnk} \in \mathbb{C}^{N_{T_q}}$ , and word embedding data symbols  $s_{qnk}$ . The transmissions occur over the resource set  $\mathcal{R}_q = \mathcal{N}_q \times \mathcal{K}_q$  with allocated subcarriers  $n \in \mathcal{N}_q$  and OFDM symbols  $k \in \mathcal{K}_q$ , with a total of  $N$  subcarriers and  $K$  symbols available. Each legitimate transmit signal propagates through the channel  $\mathbf{H}_{qnk} \in \mathbb{C}^{N_R \times N_{T_q}}$  to the server, equipped with  $N_R$  receive antennas. In this setup, an adversarial jammer aims to impair the SFL training by jamming the word embeddings in the uplink. The legitimate signal is thus corrupted by additive white Gaussian noise (AWGN)  $\boldsymbol{\eta}_{nk} \sim \mathcal{N}(\mathbf{0}, \sigma^2 \mathbf{I}) \in \mathbb{C}^{N_R}$  and by the adversarial jamming signal  $\mathbf{u}_{nk} \sim \mathcal{N}(\mathbf{0}, \mathbf{C}_{\mathbf{u}_{nk}}) \in \mathbb{C}^{N_J}$ , which propagates through the separate jamming channel  $\mathbf{G}_{nk} \in \mathbb{C}^{N_R \times N_J}$ . We define  $N_J$  as the number of jamming antennas and corresponding jamming covariance matrix as  $\mathbf{C}_{\mathbf{u}_{nk}} \in \mathbb{C}^{N_J \times N_J}$ . The receiver performs equalization using the linear filters  $\mathbf{v}_{qnk}^H \in \mathbb{C}^{1 \times N_R}$  to estimate the transmitted symbols  $\hat{s}_{qnk}$ . In summary, we have:

$$\mathbf{x}_{qnk} = \alpha_{qnk} \cdot \sqrt{p_{qnk}} \mathbf{w}_{qnk} s_{qnk} \in \mathbb{C}^{N_{T_q}}, \quad (1)$$

$$\mathbf{z}_{nk} = \mathbf{G}_{nk} \mathbf{u}_{nk} + \boldsymbol{\eta}_{nk} \in \mathbb{C}^{N_R}, \quad (2)$$

$$\mathbf{y}_{nk} = \sum_{q \in \mathcal{Q}} \mathbf{H}_{qnk} \mathbf{x}_{qnk} + \mathbf{z}_{nk} \in \mathbb{C}^{N_R}, \quad (3)$$

$$\hat{s}_{qnk} = \mathbf{v}_{qnk}^H \mathbf{y}_{nk}. \quad (4)$$

We further model  $\mathbf{H}_{qnk}$  and  $\mathbf{G}_{nk}$  as beamspace channels:

$$\mathbf{H}_{qnk} = \sum_{l=1}^{L_{H_q}} b_{H_q,l} \mathbf{a}_{N_R}(\boldsymbol{\theta}_{q,l}) \mathbf{a}_{N_{T_q}}^H(\boldsymbol{\psi}_{q,l}) e^{j2\pi\omega_{nk}(\nu_{q,l}, \tau_{q,l})} \quad (5)$$

$$\mathbf{G}_{nk} = \sum_{l=1}^{L_G} b_{G,l} \mathbf{a}_{N_R}(\boldsymbol{\theta}_{G,l}) \mathbf{a}_{N_J}^H(\boldsymbol{\psi}_{G,l}) e^{j2\pi\omega_{nk}(\nu_{G,l}, \tau_{G,l})}. \quad (6)$$

Here,  $L_{H_q}$  and  $L_G$  are the number of resolvable paths for each channel,  $b_{\cdot,l}$  is the path gain for each resolvable path  $l$ ,  $\mathbf{a}_{N_X}(\boldsymbol{\theta})$  is the steering vector at each terminal with  $N_X$  antennas,  $\boldsymbol{\theta}_{\cdot,l}$  is direction-of-arrival,  $\boldsymbol{\psi}_{\cdot,l}$  is direction-of-departure, and  $w_{nk}(\nu, \tau) = k\nu T_s - n\tau \Delta f$  is the phase shift

caused by the Doppler shift  $\nu$  and propagation delay  $\tau$ , with  $T_s$  and  $\Delta f$  being the symbol period and subcarrier spacing. Furthermore, the power  $P_q$  for each user is limited across all resource elements and the jamming signal equally adheres to a jamming power constraint  $P_J$ , i.e.

$$\sum_{(n,k) \in \mathcal{R}_q} \|\mathbf{x}_{qnk}\|_2^2 \leq P_q, \quad \sum_{(n,k) \in \mathcal{R}_q \forall q} \text{tr}(\mathbf{C}_{\mathbf{u}_{nk}}) \leq P_J. \quad (7)$$

We further assume that the legitimate parties have precise channel state information (CSI), encompassing the wireless link parameters defined by the set  $\zeta_q = \{\alpha_{qnk}, p_{qnk}, \mathbf{w}_{qnk}, \mathbf{v}_{qnk}, \mathbf{H}_{qnk}, \sigma^2\}$ . Additionally, the SFL participants are provided with the DoAs of the jamming signal, i.e.  $\boldsymbol{\theta}_G = \{\boldsymbol{\theta}_{G,l}\}_{l=1}^{L_G}$ . This may be enabled by advanced wireless sensing technologies in future 6G networks, such as integrated sensing and communication (ISAC) and reflective intelligent surfaces (RIS) [26]–[28], to name a few. Further, we assume no restrictions on the particular jamming strategy, hence the jammer is assumed to be in the so-called *jammer-dominant regime* [20] with more transmit power and antennas than any legitimate party, i.e.  $P_J \gg P_q$  and  $N_J > N_{T_q}, N_R$ . In addition, the adversary may possess full system knowledge, including  $\zeta_q$ . This represents a worst-case jammer assumption.

The adversarial jamming introduces corruption not only at the symbol level but also at the decoded message, such that jamming can be modeled as the post-decoding error as follows:

$$\hat{e}_q = e_q + \epsilon, \quad \text{where } \epsilon \sim \mathcal{N}(0, \mathbf{C}_\epsilon), \quad (8)$$

$$\text{tr}(\mathbf{C}_\epsilon) = \text{MSE}(s_q), \quad (9)$$

$$\begin{aligned} \text{MSE}(s_q) &= \mathbb{E} [\|s_q - \hat{s}_q\|_2^2] \\ &= \sum_{(n,k) \in \mathcal{R}_q} \alpha_{qnk} \cdot \mathbb{E} [|s_{qnk} - \hat{s}_{qnk}|^2]. \end{aligned} \quad (10)$$

Upon receiving the jammed signal  $\mathbf{y}_{nk}$ , the server slice continues processing the LLM attention and head layers using the corrupted word embeddings  $\hat{e}_q \neq e_q$ . At the end of the forward propagation pass, the server slice computes the training loss metric  $L: \mathbb{R}^E \rightarrow \mathbb{R}$ , which yields the corrupted loss  $L(\hat{e}_q)$  and its gradient  $\nabla L(\hat{e}_q)$ , using which the backpropagation process is initiated. This procedure is repeated for each transmission of the word embeddings across all global training rounds. We also assume that the jammer is not active in the downlink as the perturbation of gradients has been studied in various federated setups, for which corresponding defense mechanisms exist [29]. Similarly, the client- and server-side model aggregation after each global round are assumed to be unaffected by the adversary as corresponding secure aggregation strategies exist as well [30]. Note that FedAvg [9] is used in this work. Thus, the consideration of only the uplink transmission suffices to study the jamming impact on LLM word embeddings in this setup. Anti-jamming can then be directly applied if necessary conditions are fulfilled, including the assumption that maximizing the signal-to-interference-plus-noise-ratio (SINR) implies maximizing the ML performance. This assumption is verified next. Figure 2 shows the R-SFLLM system architecture, where the SFL protocol is augmented by sensing-assisted jamming DoA information, a necessary component for our anti-jamming framework in Section III.

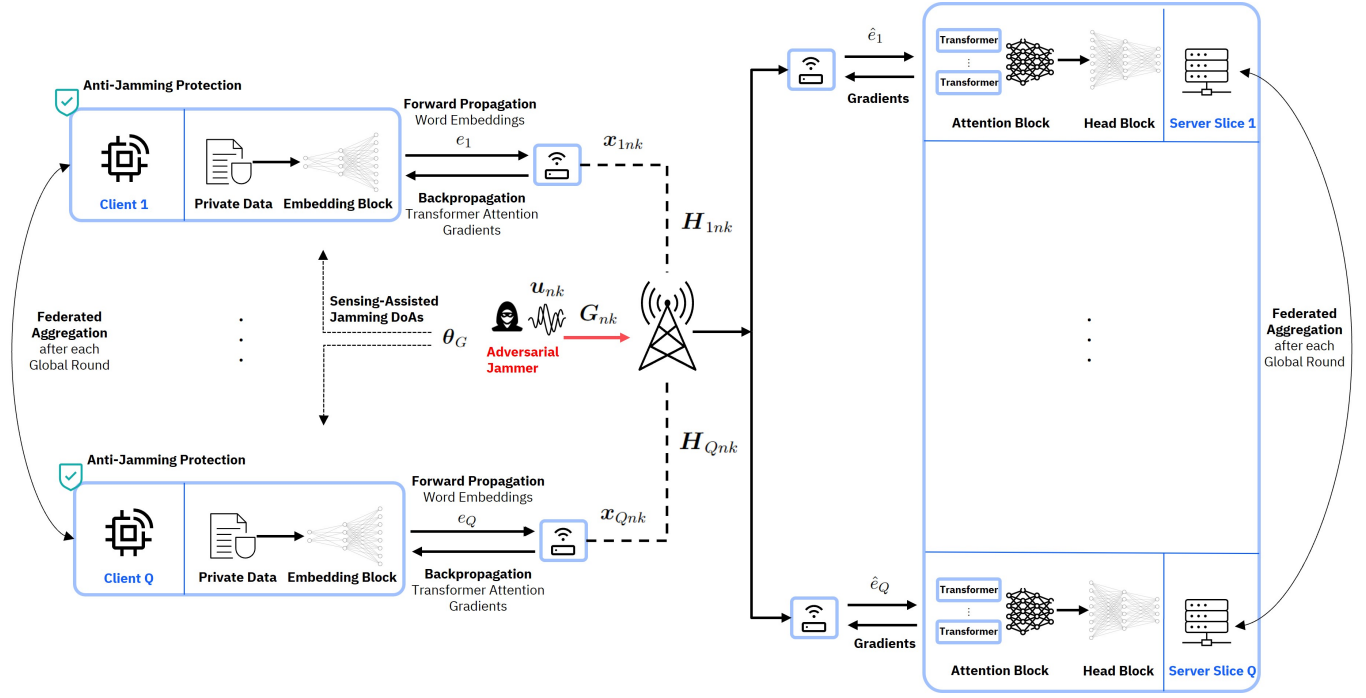


Fig. 2: R-SFLLM system architecture for distributed training over MIMO-OFDM wireless channels, augmented by sensing-assisted anti-jamming capabilities.

### B. Adversarial Jamming Impact on LLM Training in SFL

Previous works in FL typically assume the loss function to be *convex*, *twice differentiable*, and *Lipschitz smooth*. While these assumptions may hold true for simpler neural networks as in [12] and [31], more involved architectures such as transformers generally do not exhibit these properties [32]. The assumption that  $L$  is Lipschitz smooth is particularly far-reaching as this implies *bounded gradients* during backpropagation. In [33], it is shown that the standard Lipschitz assumption introduces a large variability along the optimization trajectory. Thus, a relaxed  $(\mathbf{L}_0, \mathbf{L}_1)$ -smoothness needs to be assumed, which generalizes to more complex models, such as LLMs. Based on this generalization, we derive upper bounds on the loss divergence, caused by jammed word embeddings, and show how these relate to the communication MSE.

#### 1) Assumptions on the Loss Function:

**Assumption 1.** The loss function  $L : \mathbb{R}^E \rightarrow \mathbb{R}$  is twice-differentiable and bounded from below with infimum  $L^*$ .

**Assumption 2.**  $L$  is  $(\mathbf{L}_0, \mathbf{L}_1)$ -smooth coordinate-wisely, i.e. there exist coefficient vectors  $\mathbf{L}_0, \mathbf{L}_1 \in \mathbb{R}^E$  such that for any  $\mathbf{x}, \mathbf{y} \in \mathbb{R}^E$  with  $\|\mathbf{x} - \mathbf{y}\| \leq \frac{1}{\|\mathbf{L}_1\|_\infty}$  it holds for all  $j \in [E] = \{1, \dots, E\}$  that

$$\left| \frac{\partial L(\mathbf{y})}{\partial x_j} - \frac{\partial L(\mathbf{x})}{\partial x_j} \right| \leq \left( \frac{L_{0,j}}{\sqrt{E}} + L_{1,j} \left| \frac{\partial L(\mathbf{x})}{\partial x_j} \right| \right) \cdot \|\mathbf{y} - \mathbf{x}\|_2.$$

This is a generalization of the scalar  $(L_0, L_1)$ -smoothness:

**Definition 1.**  $L$  is called  $(L_0, L_1)$ -smooth if there exist scalars  $L_0, L_1 \in \mathbb{R}$  such that for all  $\mathbf{x} \in \mathbb{R}^E$  it holds that

$$\|\nabla^2 L(\mathbf{x})\| \leq L_0 + L_1 \|\nabla L(\mathbf{x})\|.$$

The coordinate-wise  $(\mathbf{L}_0, \mathbf{L}_1)$ -smoothness implies that smoothness may vary for each coordinate of the input space.

This particularly pertains to LLMs as it has been shown in [32] that variance can be observed across mostly every transformer layer, such that each layer coordinate  $j$  satisfies an own  $(L_{0,j}, L_{1,j})$  pair. Thus, if the coefficients  $L_{1,j}$  are non-zero, smoothness is potentially *unbounded*. In contrast, if all  $L_{1,j}$  are strictly zero, the original Lipschitz smoothness is recovered. In [32], the following Lemma has been established, relating the coordinate-wise smoothness to the loss divergence.

**Lemma 1.** [32] Let  $L$  be  $(\mathbf{L}_0, \mathbf{L}_1)$ -smooth coordinate-wisely. Then for any  $\mathbf{x}, \mathbf{y} \in \mathbb{R}^E$  with  $\|\mathbf{x} - \mathbf{y}\|_2 \leq \frac{1}{\|\mathbf{L}_1\|_\infty}$ , we have

$$L(\mathbf{y}) \leq L(\mathbf{x}) + \langle \nabla L(\mathbf{x}), \mathbf{y} - \mathbf{x} \rangle + \sum_{j=1}^E \frac{\left( \frac{L_{0,j}}{\sqrt{E}} + L_{1,j} \left| \frac{\partial L(\mathbf{x})}{\partial x_j} \right| \right)}{2} \|\mathbf{y} - \mathbf{x}\|_2 |y_j - x_j|. \quad (11)$$

2) *Upper Bound on the LLM Loss Divergence:* We utilize Lemma 1 to derive the loss divergence upper bound as follows.

**Lemma 2.** For  $\mathbf{x}, \mathbf{y} \in \mathbb{R}^E$ , the loss divergence is bounded by

$$|L(\mathbf{y}) - L(\mathbf{x})| \leq \|\nabla L(\mathbf{x})\|_2 \cdot \|\mathbf{y} - \mathbf{x}\|_2 + \|\mathbf{L}_0 + \mathbf{L}_1 \odot \|\nabla L(\mathbf{x})\|_2 \cdot \|\mathbf{y} - \mathbf{x}\|_2^2. \quad (12)$$

*Proof.* See Appendix A  $\square$

In (12), the loss gradient  $\|\nabla L(\mathbf{x})\|_2$  might be unbounded, particularly when several coordinates need to be considered. However, common practice in deep learning suggests to bound gradients manually by means of gradient clipping [33] using a clipping threshold  $\tau > 0$ , thereby preventing exploding gradients, i.e.

$$\nabla L(\mathbf{x}) = \begin{cases} \nabla L(\mathbf{x}) & , \text{ if } \|\nabla L(\mathbf{x})\|_2 \leq \tau \\ \frac{\tau}{\|\nabla L(\mathbf{x})\|_2} \cdot \nabla L(\mathbf{x}) & , \text{ otherwise} \end{cases} \quad (13)$$

**Corollary 1.** If gradient clipping is applied, the upper bound on the LLM loss divergence from Lemma 2 simplifies to

$$|L(\mathbf{y}) - L(\mathbf{x})| \leq \tau \cdot \|\mathbf{y} - \mathbf{x}\|_2 + \|\mathbf{L}_0 + \tau \mathbf{L}_1\|_2 \cdot \|\mathbf{y} - \mathbf{x}\|_2^2. \quad (14)$$

Lemma 2 thus provides an upper bound on the divergence between loss functions for two distinct inputs  $\mathbf{x}$  and  $\mathbf{y}$ . This allows us to quantify the impact of adversarial jamming by measuring the loss divergence between legitimate and corrupted inputs. Corollary 1 further refines this upper bound for practical applications by incorporating gradient clipping.

3) *Relating the Model Error to the Communication MSE:* Having established the necessary upper bounds on the loss divergence, we now apply those in the context of legitimate and jammed embeddings. To this end, we first show an equivalence between the embedding MSE and the communication MSE in Proposition 1. We then use this equivalence in Proposition 2 to establish a direct relationship between the model error, expressed by the expected loss divergence, and jamming, quantifying the jammer's impact on the training performance.

**Proposition 1.** Let  $e_q, \hat{e}_q \in \mathbb{R}^E$  be the true and corrupted word embeddings and let  $s_{qnk}, \hat{s}_{qnk} \in \mathbb{C}$  be the corresponding true and corrupted transmit symbols. Then, it holds that

$$\mathbb{E} [\|e_q - \hat{e}_q\|_2^2] = \sum_{(n,k) \in \mathcal{R}_q} \alpha_{qnk} \mu_{qnk} \quad (15)$$

$$= \mathbb{E} [\|s_q - \hat{s}_q\|_2^2], \quad (16)$$

where  $\mu_{qnk}$  denotes the expected symbol error per resource allocation, i.e.

$$\mu_{qnk} = \mathbb{E} [|s_{qnk} - \hat{s}_{qnk}|^2] \quad (17)$$

$$= |p_{qnk} \mathbf{v}_{qnk}^H \mathbf{H}_{qnk} \mathbf{w}_{qnk} - 1|^2 + \mathbf{v}_{qnk}^H \mathbf{X}_{qnk} \mathbf{v}_{qnk}, \quad (18)$$

with the expectation being taken over the joint distribution of  $\{s_{qnk}\}_{(n,k) \in \mathcal{R}_q}$ ,  $\mathbf{z}_{nk}$  being conditioned on  $e_q$ , and with the interference-plus-noise covariance matrix  $\mathbf{X}_{qnk}$ , i.e.

$$\mathbf{X}_{qnk} = \sum_{q' \neq q} \mathbf{H}_{q'nk} \mathbf{b}_{q'nk} \mathbf{b}_{q'nk}^H \mathbf{H}_{q'nk}^H + \mathbf{C}_{\mathbf{z}_{nk}} \quad (19)$$

with the shorthand  $\mathbf{b}_{qnk} = \alpha_{qnk} \sqrt{p_{qnk}} \mathbf{w}_{qnk}$  and composite noise covariance  $\mathbf{C}_{\mathbf{z}_{nk}}$ .

*Proof.* The proof follows directly from  $s_{qnk}$  and  $\mathbf{z}_{qnk}$  being uncorrelated for all  $q, n, k$ , and from the assumption that we can recover  $\{s_{qnk}\}_{(n,k) \in \mathcal{R}_q}$  from  $e_{qnk}$  and vice versa.  $\square$

**Proposition 2.** Let  $L : \mathbb{R}^E \rightarrow \mathbb{R}$  satisfy Assumptions 1 and 2 with coordinate-wise smoothness parameters  $\mathbf{L}_0, \mathbf{L}_1 \in \mathbb{R}^E$  and let  $e_q, \hat{e}_q \in \mathbb{R}^E$  be the true and corrupted word embeddings with  $\|e_q - \hat{e}_q\| \leq \frac{1}{\|\mathbf{L}_1\|_\infty}$ . Then, it holds that

$$\mathbb{E} [|L(e_q) - L(\hat{e}_q)|] \leq \|\nabla_{e_q} L(e_q)\|_2 \cdot \sqrt{\mathbb{E} [\|s_q - \hat{s}_q\|_2^2]} + \|\mathbf{u}(e_q)\|_2 \cdot \mathbb{E} [\|s_q - \hat{s}_q\|_2^2], \quad (20)$$

with the expectation being taken over the joint distribution of  $\{s_{qnk}\}_{(n,k) \in \mathcal{R}_q}$ ,  $\mathbf{z}_{nk}$  being conditioned on  $e_q$ , and with

$$\mathbf{u}(e_q) = \mathbf{L}_0 + \mathbf{L}_1 \odot \nabla_{e_q} L(e_q). \quad (21)$$

*Proof.* See Appendix B  $\square$

**Corollary 2.** In the case of gradient clipping with  $\tau > 0$ , the upper bound in (20) from Proposition 2 further simplifies to

$$\mathbb{E} [|L(e_q) - L(\hat{e}_q)|] \leq \tau \cdot \sqrt{\mathbb{E} [\|s_q - \hat{s}_q\|_2^2]} + \|\mathbf{L}_0 + \tau \mathbf{L}_1\|_2 \cdot \mathbb{E} [\|s_q - \hat{s}_q\|_2^2]. \quad (22)$$

4) *Practical Interpretation of Results:* Proposition 2 provides an upper bound on the model error, defined by the expected loss divergence between legitimate and corrupted embeddings, which is *directly dependent on the MSE of the wireless communication system*. Therein, the proximity condition  $\|e_q - \hat{e}_q\|_2 \leq \frac{1}{\|\mathbf{L}_1\|_\infty}$  sets a practical constraint on the distance between legitimate and jammed embeddings, which needs to be small enough for the smoothness condition to hold. As outlined in [32], this ensures the stability of the gradient behavior, preventing numerical instabilities and unreliable approximations as gradient-dependent optimization algorithms might struggle to converge. By applying gradient clipping, we ensure that  $\|\nabla_{e_q} L(e_q)\|_2$  is bounded by  $\tau$ , thereby stabilizing the training process as the assumptions underlying the optimization methods are not violated. In particular, Corollary 2 ensures that the model error does not explode and is only dependent on the  $(\mathbf{L}_0, \mathbf{L}_1)$ -smoothness coefficients, the clipping threshold  $\tau$  and the communication MSE  $\mathbb{E} [\|s_q - \hat{s}_q\|_2^2]$ , independent of whether the proximity condition is fulfilled or not. In the context of jamming, this allows for the consideration of arbitrary adversaries, including worst-case scenarios. Hence, even if the resulting jammed word embeddings do not fulfill the proximity condition, for example due to excessive noise or sophisticated attack strategies that may flip the embedding label, our analysis remains applicable, aligning with best practices in deep learning. This new insight thus establishes a formal relationship between the transformer-based LLM architecture, its semantic word embeddings, and the wireless medium, thereby emphasizing the importance of the wireless communication system and its resilience to adversarial jamming in the quality of distributed training. To the best of our knowledge, this is the first formal characterization of such a relationship for practical DCML applications, such as SFL, with LLMs over wireless networks. In particular, we consider a generalized smoothness assumption on the loss function, which is often omitted in previous works but required for a proper analysis. This assumption explains why techniques such as gradient clipping work and may be necessary during training, and how corrupted model inputs affect the loss divergence, a critical measure for the ML training performance. Consequently, as the model error directly depends on the communication MSE, a wireless approach to resilience in SFL is not only justified but required, thus instructing us to maximize the SINR.

### C. Minimum System Rate for Reliable SFL with LLMs

To characterize the minimum system rate, under which the communication link can support SFL reliably, we need to identify outage conditions caused by jamming. To this end, we provide three remarks. In Remark 1, we first derive a lower bound for the per resource allocation symbol error. We use this

lower bound in Remark 2 to establish a general lower bound on the outage rate which is dependent on the  $\mathbf{L}_1$  constant from Lemma 1. In Remark 3, we derive the outage rate for the particular case where Proposition 2 is fulfilled with equality.

**Remark 1.** Let the resource set for each user  $q$  be defined as  $\mathcal{R}_q = \{(n, k) | \alpha_{qnk} \neq 0 \forall (n, k) \in \mathcal{R}\}$  with  $|\mathcal{R}_q| = r_q$ . For the minimum MSE (MMSE) receive filter  $v_{qnk}$  with

$$v_{qnk} = (\mathbf{X}_{qnk} + \mathbf{H}_{qnk} \mathbf{b}_{qnk} \mathbf{b}_{qnk}^H \mathbf{H}_{qnk}^H)^{-1} \mathbf{H}_{qnk} \mathbf{b}_{qnk}, \quad (23)$$

we have the following well-known equality for the per resource allocation symbol error  $\mu_{qnk}$ :

$$\mu_{qnk} = \exp\{-I(s_{qnk}, \hat{s}_{qnk})\} = \exp\{-R_{qnk}\}. \quad (24)$$

Using (24), we further have  $\mu_q = \sum_{(n,k) \in \mathcal{R}_q} \exp\{-R_{qnk}\}$ , and then, we can apply Jensen's inequality to obtain

$$\mu_q \geq r_q \cdot \exp\left\{-r_q^{-1} \sum_{(n,k) \in \mathcal{R}_q} R_{qnk}\right\} = r_q \cdot \exp\{-r_q^{-1} R_q\}. \quad (25)$$

**Remark 2.** In Proposition 2, we require  $\|e_q - \hat{e}_q\| \leq \frac{1}{\|\mathbf{L}_1\|_\infty} \forall e_q, \hat{e}_q \in \mathbb{R}^E$ , which further implies that

$$\mathbb{E}[\|e_q - \hat{e}_q\|_2^2] = \mu_q \leq \mathbb{E}[\|\mathbf{L}_1\|_\infty^{-2}] = \|\mathbf{L}_1\|_\infty^{-2}. \quad (26)$$

Using (25), we may conclude that

$$r_q \cdot \exp\{-r_q^{-1} R_q\} \leq \mu_q \leq \|\mathbf{L}_1\|_\infty^{-2}. \quad (27)$$

From here, it is easy to derive a lower bound for  $R_q$  as

$$R_q \geq r_q \cdot \log(\|\mathbf{L}_1\|_\infty^2 r_q) \stackrel{def}{=} R_{out,1}, \quad (28)$$

where  $R_{out,1}$  represents the minimum rate required for Proposition 2 to hold in its expectation.

**Remark 3.** We are interested in the rate  $R_{out,2}$ , for which (20) in Proposition 2 is fulfilled with equality. To this end, we simplify its notation for ease of analysis as follows

$$\mathbb{E}[|L(e_q) - L(\hat{e}_q)|] = \epsilon_q \leq \gamma_q \sqrt{\mu_q} + \delta_q \mu_q \quad (29)$$

where  $\epsilon_q, \gamma_q, \delta_q$  are substitutes for the corresponding expressions in (20) and  $\mu_q$  as in (25) from Remark 1. Now, we require  $\epsilon_q = \gamma_q \sqrt{\mu_q} + \delta_q \mu_q$  with equality. By setting  $y = \sqrt{\mu_q} = \sqrt{r_q \exp\{R_q/r_q\}}$ , we can equivalently state that

$$\delta_q y^2 + \gamma_q y - \epsilon_q = 0, \quad (30)$$

which has only one non-negative solution:

$$y = \frac{\gamma_q}{2\delta_q} \left( \sqrt{1 + \frac{1 + 4\gamma_q \epsilon_q}{\delta_q^2}} - 1 \right). \quad (31)$$

Thus, we obtain  $R_{out,2}$  by solving  $y^2 = r_q \cdot \exp\{R_q/r_q\}$  for  $R_q$  as

$$R_{out,2} = r_q \cdot \log(r_q/y^2). \quad (32)$$

In the context of SFL,  $R_{out,2}$  represents the rate for user  $q$  at which we can train reliably up to an error  $\epsilon_q$ .

From Remarks 2 and 3, we can conclude that both the communication system and SFL perform reliably for system

rates  $R > R_{out} = \min\{R_{out,1}, R_{out,2}\}$ . Note that the minimum rate  $R_{out}$  depends on either  $\mathbf{L}_1$  from the proximity condition or on the particular realization of the adversarial jammer captured by the MSE. Thus, particularly strong or worst-case jammers may be able to considerably decrease the system rate below  $R_{out}$ , such that neither automatic repeat requests (ARQs) nor other upper-layer resilience mechanisms can be applied. This advocates the need for proactive, resilient-by-design physical layer solutions to anti-jamming to ensure robust and reliable wireless SFL, even under worst-case conditions where reactive network defenses cannot suffice. Moreover, the proximity condition involving  $\mathbf{L}_1$  further indicates that the system can still maintain robustness if the jammer introduces only moderate noise, thereby not violating smoothness as long as the embeddings are not too divergent. This insight further opens up the door for adversarial training aspects under which robustness can even be increased due to controlled noise exposure [24], which we verify in Section IV.

### III. R-SFLLM ANTI-JAMMING FRAMEWORK

In this section, we develop the R-SFLLM anti-jamming component. To this end, we first define the anti-jamming optimization problem and provide insights into the role of sensing-assisted DoA information. Then, we solve the optimization problem using an iterative water-filling solution. Finally, we provide an analytical expression for the worst-case jamming strategy as a benchmark for our SFL resilience framework.

#### A. Anti-Jamming Strategy and Optimization Problem

As a result of Proposition 2, jammed SFL word embeddings  $\hat{e}_q$  lead to a deviation from the ground truth in the deterministic loss function  $L$ . Thus, the anti-jamming objective can be generally formulated as the minimization of the expected loss divergence, i.e.  $\min \mathbb{E}[|L(e_q) - L(\hat{e}_q)|]$ . Using Corollary 2, we can instead minimize  $J(s_q, \hat{s}_q) = \sqrt{\mathbb{E}[\|s_q - \hat{s}_q\|_2^2]} + \mathbb{E}[\|s_q - \hat{s}_q\|_2^2]$ , which is only dependent on the MSE and where we imply using gradient clipping during training. This problem can be equivalently interpreted as the maximization of the SINR for each user  $q \in \mathcal{Q}$ , respectively, or more generally, as the maximization of the sum rate. To this end, we derive an expression for the achievable sum rate as follows:

$$R = \sum_{(n,k) \in \mathcal{R}_q \forall q} I(\mathbf{y}_{nk}; \{s_{qnk}\}_{q \in \mathcal{Q}}) \quad (33)$$

$$= \sum_{(n,k) \in \mathcal{R}_q \forall q} \log \left( 1 + \sum_{q \in \mathcal{Q}} \alpha_{qnk} \rho_{qnk} \gamma_{qnk} (\mathbf{C}_{z_{nk}}) \right). \quad (34)$$

In this setup,  $\gamma_{qnk}(\mathbf{C}_{z_{nk}})$  represents the SINR of user  $q$  for the composite noise covariance matrix  $\mathbf{C}_{z_{nk}}$  and allocated resource elements  $(n, k) \in \mathcal{R}_q$ , i.e.

$$\gamma_{qnk}(\mathbf{C}_{z_{nk}}) = \mathbf{w}_{qnk}^H \mathbf{H}_{qnk}^H \mathbf{C}_{z_{nk}}^{-1} \mathbf{H}_{qnk} \mathbf{w}_{qnk}. \quad (35)$$

In order to incorporate anti-jamming in SFL by-design, we need to jointly optimize over beamforming, user scheduling, and resource allocation constraints, thus introducing resilience proactively at the bit level. To this end, we pose the following

optimization problem that is applied for all  $q \in \mathcal{Q}, n \in \mathcal{N}$ , and  $k \in \mathcal{K}$ :

$$\max_{\alpha_{qnk}, p_{qnk}, \mathbf{w}_{qnk}, \mathbf{v}_{qnk}} R \quad \text{s.t.} \quad (36)$$

$$\alpha_{qnk} \in \{0, 1\}, \quad (36a)$$

$$\alpha_{qnk} p_{qnk} \geq 0, \quad (36b)$$

$$\sum_{(n,k) \in \mathcal{R}_q} \alpha_{qnk} \leq B_q, \quad (36c)$$

$$\sum_{(n,k) \in \mathcal{R}_q} \alpha_{qnk} p_{qnk} \leq P_q, \quad (36d)$$

$$\|\mathbf{w}_{qnk}\|_2^2 \leq 1. \quad (36e)$$

In this problem, constraints (36a) to (36c) incorporate the binary user scheduling, power allocation and resource block limitation, with  $B_q = |\mathcal{R}_q|$  being the maximum number of resource allocation blocks for each user  $q$ . Constraint (36d) captures the power budget and constraint (36e) ensures the unit normalization of the beamforming vector. However, due to the binary user scheduling variable  $\alpha_{qnk}$ , the optimization is a non-linear, non-convex mixed-integer problem and thus NP-hard in general. In addition to NP-hardness, the sum rate further depends on the composite noise covariance matrix  $\mathbf{C}_{z_{nk}}$ . Since the latter characterizes the adversarial jamming strategy, which is not known to the legitimate SFL parties, a surrogate expression  $\tilde{\mathbf{C}}_{z_{nk}}$  needs to be found, which effectively approximates the true covariance, i.e.  $\tilde{\mathbf{C}}_{z_{nk}} \approx \mathbf{C}_{z_{nk}}$ .

### B. Role of Sensing-Assisted Jamming DoA Information

We have shown in [34] that such a surrogate covariance can be approximated using the jamming signal DoAs as follows:

$$\tilde{\mathbf{C}}_{z_{nk}} = \eta \mathbf{A}(\boldsymbol{\theta}_G) \mathbf{A}(\boldsymbol{\theta}_G)^H + \sigma^2 \mathbf{I}_{N_R} \succeq \mathbf{C}_{z_{nk}} \quad (37)$$

with the array manifold evaluated at the known DoAs, i.e.

$$\mathbf{A}(\boldsymbol{\theta}_G) = [\mathbf{a}_{N_R}(\boldsymbol{\theta}_{G,1}) \dots \mathbf{a}_{N_R}(\boldsymbol{\theta}_{G,L_G})]. \quad (38)$$

This was motivated by showing that the true SINR  $\gamma$  can be lower bounded by an approximate expression  $\tilde{\gamma}$ , which is dependent on a scaling parameter  $\eta$  and the DoAs as follows:

$$\gamma(\mathbf{w}, \mathbf{v}) \geq \frac{\mathbf{v}^H \mathbf{H} \mathbf{w} \mathbf{w}^H \mathbf{H}^H \mathbf{v}}{\mathbf{v}^H (\eta \mathbf{A}_{R_x}(\boldsymbol{\theta}_G) \mathbf{A}_{R_x}(\boldsymbol{\theta}_G)^H + \sigma^2 \mathbf{I}) \mathbf{v}} \stackrel{\text{def}}{=} \tilde{\gamma}(\mathbf{w}, \mathbf{v}). \quad (39)$$

By inserting (37) into (34), we hence obtain a lower bound on  $R$ . Note that in general  $\eta$  is unknown since it depends on the unknown jamming setup. Thus, we consider it as a hyper-parameter, which controls the resilience level of our system. In [34], we showed that by choosing  $\eta$  to be much larger than the noise level  $\sigma^2$ , i.e.  $\eta \gg \sigma^2$ , we coincide with the case where the jammer setup is known, that is where  $\gamma \approx \tilde{\gamma}$ . In this case, the SINR can be maximized by maximizing the lower bound  $\tilde{\gamma}$  instead. Thus,  $\tilde{\mathbf{C}}_{z_{nk}}$  constitutes a conservative approximation of  $\mathbf{C}_{z_{nk}}$ , ensuring it does not underestimate the impact of noise and adversarial jamming, indicated by the Löwner order  $\succeq$  in (37). We carefully validated this conjecture in [22] for  $\eta = 10$  in several jamming scenarios for a range of power budgets  $P_J < \infty$ . Consequently, the availability of the DoAs alleviates the need to know the exact jamming statistics.

---

### Algorithm 1: Joint Iterative Scheduling, Beamforming, and Power Allocation

---

**Input:** Legitimate channel  $\mathbf{H}_{qnk}$ , noise covariance  $\mathbf{C}_{z_{nk}}$ , power constraint  $P_q$ , maximum number of resource allocation blocks  $B_q$

**Output:** Wireless system design variables  $\alpha_{qnk}, p_{qnk}, \mathbf{w}_{qnk}$

---

- 1 Initialize the interference-plus-noise covariance matrix to  $\mathbf{X}_{qnk} = \mathbf{C}_{z_{nk}}$
  - 2 Initialize the design variables  $\alpha_{qnk}^0, p_{qnk}^0, \mathbf{w}_{qnk}^0$  using the single user update procedure in steps (6)-(11)
  - 3 **while not converged do**
  - 4     **for**  $q = 1$  to  $Q$  **do**
  - 5         Update  $\mathbf{X}_{qnk}$  using Equation (19)
  - 6         Compute the *maximum eigenvalues*  $\{\lambda_{qnk}\}_{(n,k) \in \mathcal{R}_q}$  of  $\{\mathbf{H}_{qnk}^H \mathbf{X}_{qnk}^{-1} \mathbf{H}_{qnk}\}_{(n,k) \in \mathcal{R}_q}$
  - 7         Compute the corresponding eigenvectors  $\{\mathbf{u}_{qnk}\}_{(n,k) \in \mathcal{R}_q}$
  - 8         Determine the indices  $\mathcal{I}_q$  of the largest  $B_q$  eigenvalues
  - 9         Set the user scheduling to  $\alpha_{qnk} = 1$  for all  $(n, k) \in \mathcal{I}_q$  and 0 otherwise
  - 10         Compute the power allocation  $p_{qnk} = (\mu - \lambda_{qnk}^{-1})^+$  with  $\mu$  chosen such that  $\sum_{\mathcal{I}_q} p_{qnk} \leq P_q$
  - 11         Set the beamforming vector to  $\mathbf{w}_{qnk} = \mathbf{u}_{qnk}$  for  $(n, k) \in \mathcal{I}_q$
- 

### C. Iterative Water-Filling Solution

We have further shown in [22] that the NP-hard problem in (36) can be iteratively solved using a water-filling approach, as described in Algorithm 1. The proposed method adapts the original water-filling for MAC and MIMO channels [35] to incorporate user scheduling. To this end, each user  $q \in \mathcal{Q}$  determines its update on the matrix  $\mathbf{X}_{qnk}$  and computes an optimal set of the wireless system design parameters  $\alpha_{qnk}, p_{qnk}, \mathbf{w}_{qnk}$ , as outlined in steps (6)-(11), where for each user the following optimization problem is solved:

$$\max_{\alpha_{qnk}, p_{qnk}, \mathbf{w}_{qnk}} \sum_{(n,k) \in \mathcal{R}_q} \underbrace{\alpha_{qnk} \cdot \log(1 + p_{qnk} \gamma_{qnk}(\mathbf{X}_{qnk}))}_{R_q}. \quad (40)$$

Algorithm 1 effectively circumvents the need to deal with the NP-hardness of the problem as the overall sum rate is indirectly maximized by maximizing the sum rate  $R_q$  of the strongest users individually. In each iteration, we use the power iteration method for computing eigenvalues and eigenvectors, and perform water-filling for power allocation. Both of these methods are known to exhibit rapid convergence. Consequently, Algorithm 1 inherits these convergence properties, which we have verified in extensive experiments, where our method on average takes less than five iterations to converge. With  $n_{\text{iter}}$  representing the number of iterations required for convergence, the overall complexity of the algorithm is

$$\mathcal{O}(n_{\text{iter}} Q N K N_R N_T^2). \quad (41)$$

### D. Worst-Case Jamming Strategy

In Proposition 2, we have seen that jamming LLM word embeddings affects the training performance. However, the impact still remains to be investigated for worst-case conditions and in particular how this affects the global performance in SFL after aggregating such corrupted models. To this end, we need to derive the worst-case jamming strategy, which we use to benchmark R-SFLLM. In contrast to anti-jamming, we

**Algorithm 2:** Approximate Worst-Case Jamming Strategy

**Input:** Legitimate channel  $\mathbf{H}_{qnk}$ , jamming channel  $\mathbf{G}_{nk}$ , jamming power budget  $P_J$

**Output:** Worst-case jamming covariance matrix  $\mathbf{C}_{u_{nk}}$

---

```

1 for each user  $q \in \mathcal{Q}$  do
2   Compute the alignment matrix
    $\mathbf{R}_{qnk} = \mathbf{G}_{nk}^\dagger \mathbf{H}_{qnk} \mathbf{H}_{qnk}^H \mathbf{G}_{nk}^\dagger, H$ 
3 Determine the strongest user  $q^* = \arg \max_{q \in \mathcal{Q}} \lambda_{\max}(\mathbf{R}_{qnk})$ 
4 for the strongest user alignment  $\mathbf{R}_{q^*nk}$  do
5   Compute the eigenvector matrix  $\mathbf{U}_{q^*nk}$  and eigenvalues
    $\{\lambda_{q^*nk,d}\}_{d=1}^{N_J}$ 
6 Compute the jamming power allocation weighting
    $h_{nk} = p_{q^*nk} \sum_{d=1}^{N_J} \lambda_{q^*nk,d}$ 
7 Compute the jamming power scaling factors
    $g_{nk} = (P_J \sqrt{h_{nk}}) / (\sum_{nk} \sqrt{h_{nk}})$ 
8 Compute the jamming power allocation matrix
    $\mathbf{A}_{u_{nk}} = \text{diag} \left\{ \frac{g_{nk} \lambda_{q^*nk,d}}{\sum_{d=1}^{N_J} \lambda_{q^*nk,d}} \right\}_{d=1}^{N_J}$ 
9 Compute the jamming covariance matrix
    $\mathbf{C}_{u_{nk}} = \mathbf{U}_{q^*nk} \mathbf{A}_{u_{nk}} \mathbf{U}_{q^*nk}^H$ 

```

---

need to find the covariance matrix  $\mathbf{C}_{u_{nk}}$ , which minimizes  $R$  instead, and pose the following adversarial objective:

$$\min_{\mathbf{C}_{u_{nk}}} R \quad \text{s.t.} \quad \forall (n, k) \in \mathcal{R}_q \quad (42)$$

$$\mathbf{C}_{u_{nk}} = \mathbf{C}_{u_{nk}}^H, \quad (42a)$$

$$\mathbf{C}_{u_{nk}} \succeq \mathbf{0}, \quad (42b)$$

$$\sum_{(n,k) \in \mathcal{R}_q} \text{tr}(\mathbf{C}_{u_{nk}}) \leq P_J. \quad (42c)$$

This is a convex semidefinite program due to the objective function and the constraints being convex. Thus, a global optimum can be found in polynomial time using interior-point or first-order methods [36]. However, neither one of these approaches scales efficiently for high-dimensions with a complexity of  $\mathcal{O}(N_J^4 N^2 K^2)$ , or higher [37]. Thus, we require a compute-efficient alternative. To this end, we proposed a two-step approximation procedure in [22] described in Algorithm 2, which consists of a prior user selection stage and a subsequent compute-efficient convex optimization. In [22], we have further shown that this worst-case jammer nullifies the sum rate, independent of the number of antennas and DoAs. Thus, we adopt this adversary as a benchmark in the subsequent experiments and investigate its impact on the global model performance in SFL with LLMs to answer the question whether worst-case jamming translates into worst-case SFL training performance.

#### IV. EXPERIMENTS, SIMULATION RESULTS AND ANALYSIS

In this section, we discuss our simulation results for applying R-SFLLM to the distributed training of LLMs. We provide insights into the sensitivity of SFL to poisoned LLM aggregations, the impact of the worst-case jammer as compared to barrage jamming, the effectiveness of sensing-assisted anti-jamming, as well as the role of different LLM architectures.

#### A. Experimental Setup

We refer to the R-SFLLM setup in Figure 2. Therein,  $Q = 3$  legitimate clients participate in *fine-tuning* BERT [38] and RoBERTa [39] base models for two distinct NLP tasks: Sequence classification (SC) and named entity recognition (NER). SC assigns a category to a sequence of words or tokens, while NER identifies named entities, such as persons or organizations within a text. For SC, the binary classification datasets SST2 [40] and QNLI [41], as well as the ternary dataset MNLI [42] are considered, while for NER the CONLL2003 [43] and WNUT17 [44] datasets are used. Each dataset is divided equally among the clients, ensuring a unique and private portion of the data. For each NLP task, the pre-trained LLMs are fine-tuned for  $N_{\text{epochs}} = 10$  epochs and  $N_{\text{rounds}} = 10$  global SFL rounds. In this setup, worst-case adversarial jamming is encountered during each uplink transmission of the LLM word embeddings in the MIMO-OFDM MAC. All participating parties employ uniform linear antenna arrays with  $N_{T_q} = 8$  and  $N_R = 16$  legitimate transmit and receive antennas. The adversary is assumed to be in the jammer-dominant regime and employs the previous worst-case strategy to maximally corrupt the LLM word embeddings. The corresponding user and jamming DoAs are determined as

$$\theta_{H_{q,l}} = \theta_{H_q} + \phi_{H_{q,l}} \quad \text{and} \quad \theta_{G,l} = \theta_J + \phi_{G,l} \quad (43)$$

where the central angles  $\theta_{H_q}$  and  $\theta_J$  are set to  $0^\circ$  and  $20^\circ$ , respectively. The disturbance in form of the angle spread  $\phi_{\cdot,l}$  for each antenna  $l$  is drawn uniformly via  $\mathcal{U}(\cdot)$  according to

$$\phi_{H_{q,l}} \sim \mathcal{U}[-10^\circ, 10^\circ] \quad \text{and} \quad \phi_{G,l} \sim \mathcal{U}[-5^\circ, 5^\circ]. \quad (44)$$

The considered communication protocol employs 5G New Radio (NR) slots with  $K = 14$  symbols per slot and  $N = 64$  subcarriers. The maximum number of resource allocation blocks for each user  $q$  is given by  $B_q = \lfloor \frac{NK}{Q} \rfloor = 298$ .

We choose the scale parameter of the sensing-assisted R-SFLLM anti-jamming to be  $\eta = 10$ , which is similar to previous experiments in [22] and hence much larger than the background noise  $\sigma^2 = -3$  dBm. We further resample the jamming statistics after each uplink transmission, i.e. after each training batch, to simulate movement and jamming variance. The following four scenarios are studied as benchmarks:

- 1) *SFL Baseline*: SFL performance without wireless model.
- 2) *Gaussian*: No adversarial jamming, only AWGN.
- 3) *No Protection*: Worst-case jamming without R-SFLLM.
- 4) *Protection*: Worst-case jamming with R-SFLLM.

Table I summarizes the experiment configuration and Table II shows the fine-tuning results for each scenario. We further include detailed performance plots for the aggregated global SFL model after each global round, i.e. after each  $N_{\text{epochs}}$ , for every dataset, base model, and scenario in Figure 3.

#### B. R-SFLLM Simulation Results

1) *Sequence Classification*: As shown in Table II, for all three SC datasets, R-SFLLM is able to consistently safeguard the distributed training in general, leading to robust global models with classification accuracies near-identical or very

| Wireless Configuration Parameters      |   |   |
|--|---|---|
| $Q$                                    | Number of legitimate users                                | 3   |
| $N_{T_q}$                              | Number of legitimate transmit antennas per user           | 8   |
| $N_R$                                  | Number of legitimate receive antennas at the base station | 16  |
| $N_J$                                  | Number of jammer transmit antennas                        | 64  |
| $P_J$                                  | Jamming power   | 30 dBm                                      |
| $P_q$                                  | Power of legitimate user $q$                              | 5 dBm                                       |
| $\theta_{H_{q,l}}$                     | DoA for legitimate users                                  | $\theta_{H_q} + \phi_l$                     |
| $\theta_{G,l}$                         | DoA for adversarial jammer                                | $\theta_J + \phi_l$                         |
| $\theta_{H_q}$                         | Central DoA for legitimate user                           | $0^\circ$                                   |
| $\theta_J$                             | Central DoA for adversarial jammer                        | $20^\circ$                                  |
| $\phi_{H_{q,l}}$                       | Angle spread for legitimate users                         | $\pm 10^\circ$                              |
| $\phi_{G,l}$                           | Angle spread for adversarial jammer                       | $\pm 5^\circ$                               |
| $K$                                    | Symbols per LTE-like slot                                 | 14  |
| $N$                                    | Subcarriers   | 64  |
| $B_q$                                  | Maximum number of resource blocks for user $q$            | $\lfloor \frac{N \cdot K}{Q} \rfloor = 298$ |
| $\eta$                                 | Scale parameter of anti-jamming framework                 | 10  |
| $\sigma^2$                             | Background noise  | -3 dBm                                      |
| Path loss                              | Path loss   | 10 dB                                       |
| Number of paths                        | Number of propagation paths                               | 128   |
| $f_c$                                  | Carrier frequency   | 2.4 GHz                                     |
| SFL Training Parameters                |   |   |
| $N_{\text{epochs}}, N_{\text{rounds}}$ | Number of training epochs & global SFL rounds             | 10  |
| $b_{\text{SST2\_MNLI}}$                | Batch Size for the SST2 & MNLI dataset                    | 64  |
| $b_{\text{QNLI}}$                      | Batch Size for the QNLI dataset                           | 32  |
| $b_{\text{CONLL2003}}$                 | Batch Size for the CONLL2003 dataset                      | 16  |
| $b_{\text{WNUT17}}$                    | Batch Size for the WNUT_17 dataset                        | 4   |
| $\alpha$                               | Learning rate   | 1e-5  |
| $\epsilon$                             | ADAM numerical stability constant                         | 1e-6  |
| $P_{\text{WARMUP}}$                    | Warmup period in percent of iterations                    | 10%   |

TABLE I: Summary of SFL and wireless configuration parameters.

|                     | SFL Baseline | Gaussian | Protection | No Protection |
|---------------------|--------------|----------|------------|---------------|
| SST2 (BERT)         | 91.9%        | 91.2%    | 92.3%      | 50.9%         |
| SST2 (RoBERTa)      | 93.2%        | 93.8%    | 93.0%      | 50.9%         |
| QNLI (BERT)         | 87.9%        | 87.8%    | 88.0%      | 50.5%         |
| QNLI (RoBERTa)      | 91.5%        | 91.0%    | 87.1%      | 49.5%         |
| MNLI (BERT)         | 80.8%        | 81.6%    | 81.5%      | 35.4%         |
| MNLI (RoBERTa)      | 86.0%        | 85.7%    | 82.5%      | 33.2%         |
| CONLL2003 (BERT)    | 92.2%        | 92.5%    | 92.7%      | 10.1%         |
| CONLL2003 (RoBERTa) | 93.6%        | 93.2%    | 89.5%      | 9.7%          |
| WNUT17 (BERT)       | 58.5%        | 54.8%    | 51.7%      | 26.3%         |
| WNUT17 (RoBERTa)    | 54.1%        | 53.8%    | 43.7%      | 23.1%         |
| Client 1 MSE        | $-\infty$ dB | -10.2 dB | -7.9 dB    | 23.3 dB       |
| Client 2 MSE        | $-\infty$ dB | -9.8 dB  | -5.9 dB    | 25.9 dB       |
| Client 3 MSE        | $-\infty$ dB | -10.5 dB | -3.4 dB    | 27.1 dB       |

TABLE II: Fine-Tuning results for BERT and RoBERTa on SST2, QNLI, MNLI, CONLL2003, and WNUT17 datasets across different SFL training scenarios, evaluated via Accuracy (for SC) and F1 Scores (for NER).

close to the baselines. For instance, BERT achieves near-identical performance to the SST2 baseline with accuracies above 91% for the scenarios when worst-case jamming is absent (*Gaussian*) and when R-SFLLM protection against it is employed (*Protection*). This indicates that AWGN alone does not significantly impact the word embeddings and is negligible within a statistical variance, thereby acting as a light regularizer. As for the scenario where no protection is provided (*No Protection*), the worst-case jammer is successful in maximally disrupting the distributed training, resulting in a global model accuracy of around 50%. As such, the global SFL model is no better than simple guessing, in other words, it has not been able to learn anything and subsequently has worst-case binary classification performance. This answers the question of whether worst-case jamming translates into worst-case performance positively. Moreover, each client observes near optimal performance from early epochs on, such that the global model already converges after the first global round as shown in Figure 3a. The same can be observed for MNLI and QNLI in Figures 3c and 3d. Hence, we can state that BERT is already well pre-trained on sentiment analysis, such that SC might be an easy fine-tuning task.

In comparison, RoBERTa achieves a slightly better overall baseline performance around 93% for SST2, indicating a potential advantage due to its more complex architecture. However, for the scenario *Protection*, Figure 3b shows that the global model starts off with a slightly lower accuracy and converges to the baseline after the second global round. While negligible in this case, this may indicate that RoBERTa might be more sensitive to noisy embeddings. This is due to the fact that jamming cannot be mitigated perfectly, resulting in higher MSEs for scenario *Protection* as compared to *Gaussian*. A possible explanation is that RoBERTa does not use segment embeddings and relies solely on position and token embeddings, unlike BERT, which uses all three embedding types. Furthermore, RoBERTa’s pre-training process involves more extensive and diverse data, leading to a model that is more finely tuned to the nuances of language. This renders RoBERTa more susceptible to perturbations in the word embeddings, as it has learned to rely on subtle features that can be disrupted by noise. This noise sensitivity is more pronounced for the QNLI and partly for the MNLI dataset in Figures 3f and 3d, respectively. In particular, RoBERTa converges to the QNLI baseline only after the sixth global round.

Figure 4 further shows the QNLI performance for RoBERTa clients 1 to 3, respectively, where clients 1 and 2 approach the baseline whereas client 3 aligns more to the observed global SFL model. When further comparing the MSEs for each user in Table II, client 1 experiences the lowest MSE, while client 3 experiences the highest MSE, which is about 2.8 times higher than the one from client 1. This indicates that the developed resource allocation of the proposed protection scheme is not fair. However, this difference, while significant, does not seem to particularly affect the BERT model. This corroborates that RoBERTa is more sensitive to noisy word embeddings in general. However, since this is not necessarily observed for RoBERTa on the SST2 dataset, there likely is an additional dependence on the data distribution, such that a potentially non-independently-and-identically distributed (non-IID) data split may further decrease the performance in case of corrupted word embeddings. Thus, fine-tuning RoBERTa may result in an initially worse model if some clients underperform.

Nevertheless, R-SFLLM remains successful in mitigating the worst-case jammer, albeit after a few global rounds. This further indicates that RoBERTa makes use of the adversarial noise and robustifies over the training period, thus benefitting from the adversarial training character of R-SFLLM, in which the additional noise, if moderate, helps the model to regularize over time, thereby managing to yield a close-to-optimal global model performance after a few global rounds. This is similar to traditional adversarial training [45], however targets only word embeddings and no other layers instead.

2) *Named Entity Recognition*: Table II shows that BERT similarly achieves near-identical performance to the SFL baseline for CONLL2003 with F1 scores above 92% for the scenarios *Gaussian* and *Protection*. Again, *No Protection* results in maximal disruption, with consistent F1 scores around 10%. This suggests that the model is either missing almost all of the entities (low recall) or predicting almost all entities incorrectly (low precision), which ultimately renders the obtained global

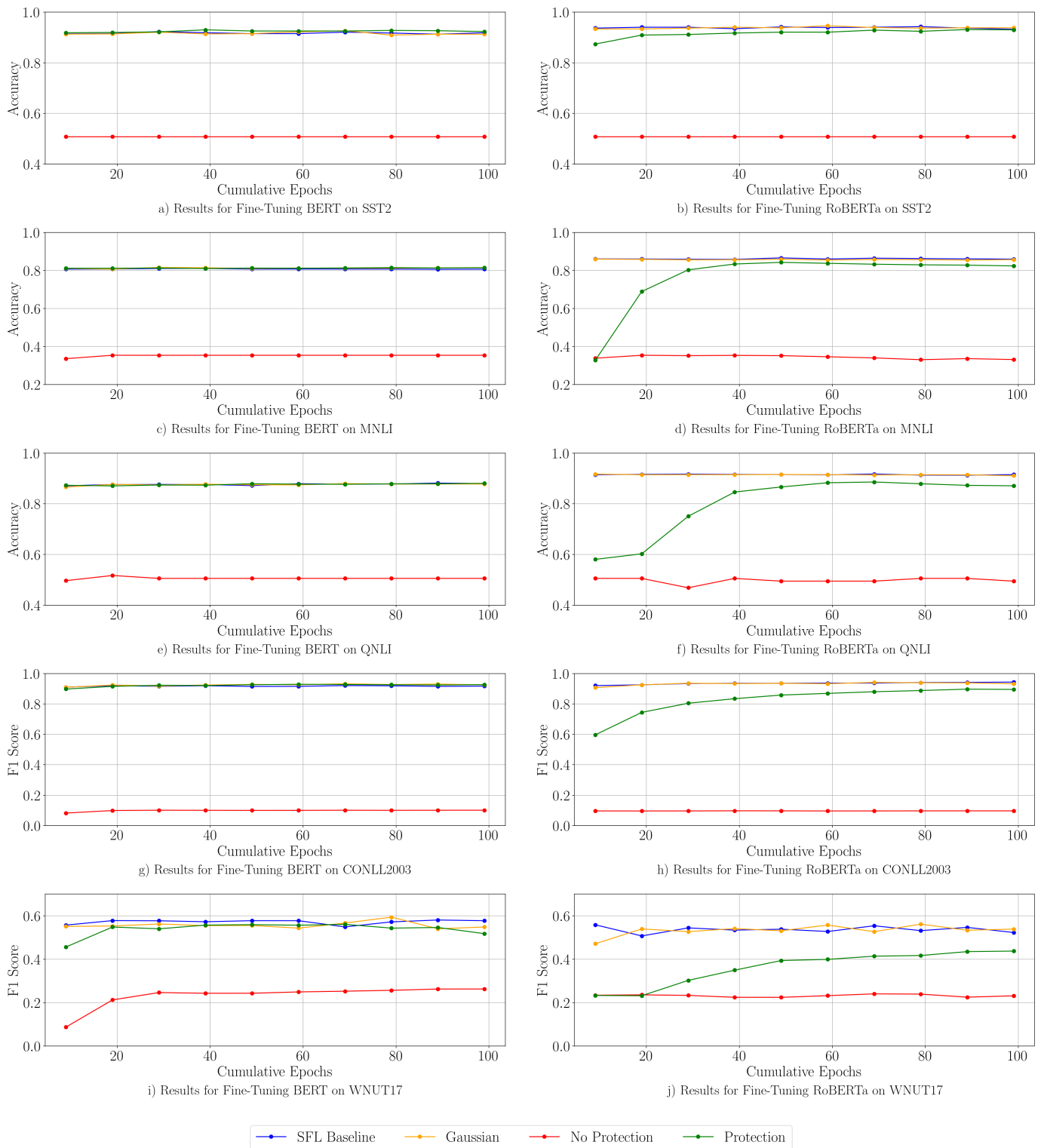


Fig. 3: Global SFL model performance plots, evaluated after each of the  $N_{\text{rounds}}$  global rounds for all four scenarios (SFL Baseline, Gaussian, No Protection, Protection) using Accuracy and F1 Scores (higher is better). Accuracy is calculated as the ratio of correctly classified sentences/words to the total number of instances, while the F1 Score is the harmonic mean of precision (the ratio of true positive observations to the total number of predicted positives) and recall (the ratio of true positive observations to the number of actual positives, i.e. the sum of true positives and false negatives).

model unusable for NER. Thus, worst-case jamming results in worst-case model performance. In addition, Figure 3g again shows that each client observes near optimal performance from early epochs on. This further corroborates the assumption that the BERT architecture is robust against noisy embeddings due to potentially unfair resource allocation in wireless SFL.

RoBERTa achieves similar outcomes for CONLL2003 with near-identical performance to the original baseline with F1 scores of around 93%. Worst-case global model performance is observed for the scenario *No Protection* with F1 scores around 10% as well. However, as observed for SC, the global SFL model for scenario *Protection* starts out at lower F1 scores around 60% and converges gradually to the baseline toward the end of the global training as shown in Figure 3h. This observation can be attributed to the same argumentation as before, in which the RoBERTa base model seems to be more vulnerable to noise in word embeddings, especially if some clients are subjected to higher MSEs due to unfair resource allocation. Thus, similarly as for SC, the global SFL model performance converges to the original baseline after a few global rounds, where RoBERTa makes use of the adversarial training property and robustifies over the fine-tuning period.

In contrast to CONLL2003, WNUT17 represents a more challenging dataset, which not only exhibits a significantly lower baseline performance for non-distributed training, but also consists of only few samples, such that each client is challenged with poorer insights into the data. However, even in this case, BERT achieves good but not great performance for all relevant scenarios given the small dataset. Furthermore, the worst-case jammer is able to successfully impair the global model with F1 scores around 25%, which corresponds to the performance of the baseline after only one epoch as shown in Figure 3i. Accordingly, the global model in this case continues to miss almost all of the entities, having not progressed at all.

Furthermore, RoBERTa’s sensitivity to noisy word embeddings becomes more pronounced when dealing with particularly small datasets. Specifically, Figure 5 shows that while clients 1 and 2 achieve the baseline performance, client 3 with higher MSE does not. This results in a worse performing global model as shown in Figure 3j, where the projected performance trajectory indicates that RoBERTa not only needs more data but also more global training rounds to successfully mitigate the worst-case jamming impact. However, the performance after 10 global rounds is already remarkably better than in the case where no R-SFLLM protection is applied. These results suggest that both BERT and RoBERTa become more susceptible to noisy embeddings in wireless SFL when small datasets with potentially non-representative samples are used for training. The model might thus not generalize well nor benefit from the adversarial training feature of R-SFLLM.

3) *Jamming only one User*: Based on the previous discussions and the results in Figures 4 and 5, it suffices if only one SFL party performs suboptimal for the global model to decrease in performance. However, this was investigated under the setting that all SFL clients are jammed simultaneously and where always client 3 suffered from higher MSEs due to unfair resource allocation as a result of our water-filling approach. To extend the investigation, Figure 6 provides simulation results

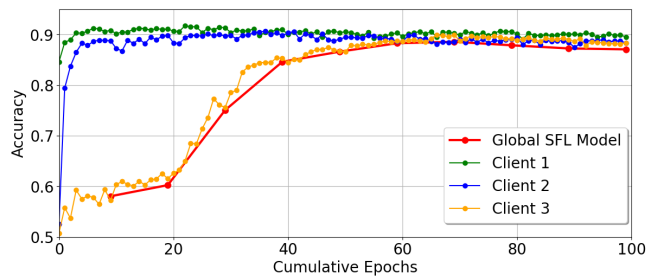


Fig. 4: Results for fine-tuning RoBERTa on QNLI with all client plots.

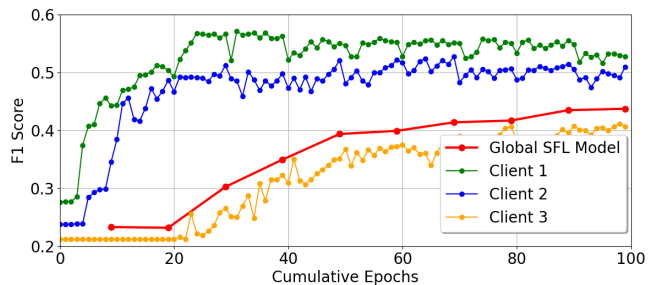


Fig. 5: Results for fine-tuning RoBERTa on WNUT17 with all client plots.

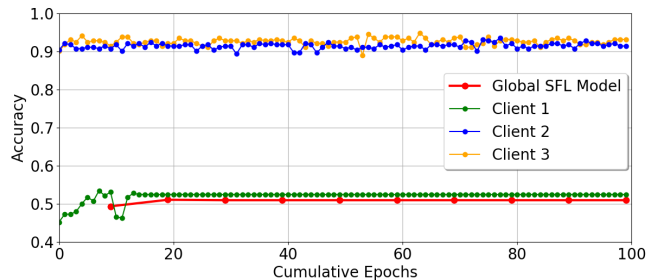


Fig. 6: Results for fine-tuning BERT on SST2 when jamming only client 1. The global SFL model cannot recover even if only one party is targeted.

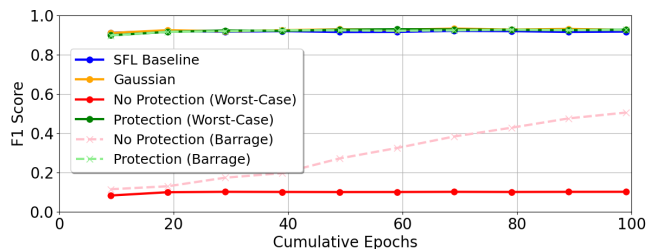


Fig. 7: Results for fine-tuning BERT on CONLL2003 with additional barrage jamming. The worst-case jammer is consistently stronger over all epochs and global SFL rounds while the barrage jammer improves gradually over time.

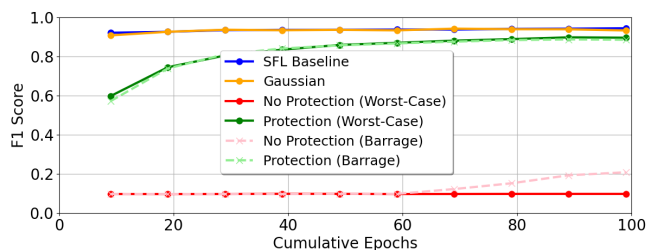


Fig. 8: Results for fine-tuning RoBERTa on CONLL2003 with additional barrage jamming. The worst-case jammer is consistently stronger over all epochs and global SFL rounds while the barrage jammer improves only marginally after the sixth round.

for BERT on SST2, where only one party (client 1) is jammed and shows that SFL is highly sensitive to aggregating even only one (randomly) poisoned model, regardless of whether BERT is more robust against noisy embeddings. Note that similar worst-case results can be obtained for RoBERTa, other datasets and other clients. This further corroborates the findings in [14], where it was shown that few poisoned clients already compromise the global model. We thus show that this can be achieved via jamming attacks in wireless SFL.

4) *Barrage Jamming*: Next, we quantify how adversaries other than worst-case jammers affect the SFL performance. To this end, we employ a barrage jammer with covariance  $C_{\mathbf{u}_{n,k}} = P_J/(N_J N K)$  and demonstrate results for BERT and RoBERTa on CONLL2003 in Figures 7 and 8, respectively. In both cases, barrage jamming has a non-negligible impact on the performance for scenario *No Protection*, which at first resembles the worst-case but improves with later global rounds. For BERT, SFL performance gradually increases with every global round and achieves an F1 score of 51%, which is still 41% less than the baseline. For RoBERTa, performance, increases only marginally after the sixth round and achieves an F1 score of 21%, being only 11% higher than the worst-case. This is interesting as clients 1,2 and 3 observe MSEs of 5.3dB, 8.0dB and 9.2dB, respectively, which are significantly lower than for the worst-case but slightly higher than for scenario *Protection*. This indicates a nonlinear and architecture-dependent relationship where small noise acts as a regularizer but higher noise beyond a certain threshold results in severe corruption, particularly for noise-sensitive RoBERTa models. Nevertheless, only the worst-case jammer is able to consistently maintain its detrimental performance. As for scenario *Protection*, barrage jamming matches the previous experiments. Thus, R-SFLLM mitigates adversarial jamming with equal performance, regardless of whether worst-case, barrage, or consequently any other jammer is employed.

## V. CONCLUSION

In this paper, we have investigated the problem of adversarial jamming attacks in wireless SFL with LLMs. We have demonstrated both theoretically and experimentally that jamming LLM word embeddings leads to significantly worse model outcomes. Specifically, we have shown that worst-case jamming results in worst-case performance across all SFL rounds, regardless of how many clients are being targeted. To address this, we have proposed R-SFLLM, a sensing-assisted anti-jamming framework that leverages information about the adversary's DoAs to integrate resilience directly into the wireless system by design. We have justified this wireless approach to resilience by showing that the LLM model error is upper bounded by the communication MSE under a relaxed  $(L_0, L_1)$  smoothness assumption, thereby emphasizing that the physical layer directly impacts the training. Extensive experiments validate the effectiveness of R-SFLLM and demonstrate the critical need to safeguard LLM word embeddings in SFL against jamming attacks to ensure model integrity in distributed training over wireless networks.

## APPENDIX A PROOF OF PROPOSITION 1

First, we adapt the original proof for Lemma 1 in [32] and reformulate its initial statement toward the loss divergence:

$$L(\mathbf{y}) - L(\mathbf{x}) = \nabla L(\mathbf{x})^T (\mathbf{y} - \mathbf{x}) + \int_0^1 \langle \nabla L(\mathbf{x} + u(\mathbf{y} - \mathbf{x})) - \nabla L(\mathbf{x}), \mathbf{y} - \mathbf{x} \rangle du. \quad (45)$$

Second, applying the norm  $|\cdot|$  and triangle inequality yields

$$|L(\mathbf{y}) - L(\mathbf{x})| \leq |\nabla L(\mathbf{x})^T (\mathbf{y} - \mathbf{x})| + \left| \int_0^1 \langle \nabla L(\mathbf{x} + u(\mathbf{y} - \mathbf{x})) - \nabla L(\mathbf{x}), \mathbf{y} - \mathbf{x} \rangle du \right|. \quad (46)$$

Third, we use the upper bound on this integral from the proof in [32] to further obtain

$$|L(\mathbf{y}) - L(\mathbf{x})| \leq |\nabla L(\mathbf{x})^T (\mathbf{y} - \mathbf{x})| + \left| \sum_{j=1}^E \left[ L_{0,j} + L_{1,j} \left| \frac{\partial L(\mathbf{x})}{\partial x_j} \right| \right] |y_j - x_j| \cdot \|\mathbf{y} - \mathbf{x}\|_2 \right|. \quad (47)$$

By defining the vectors  $\mathbf{u} = [u_1 \dots u_E]^T$  with  $u_j = L_{0,j} + L_{1,j} \left| \frac{\partial L(\mathbf{x})}{\partial x_j} \right|$  and  $\mathbf{v} = [v_1 \dots v_E]^T$  with  $v_j = |y_j - x_j|$ , above expression can be denoted via scalar products, i.e.

$$|L(\mathbf{y}) - L(\mathbf{x})| \leq |\nabla L(\mathbf{x})^T (\mathbf{y} - \mathbf{x})| + |\mathbf{u}^T \mathbf{v} \cdot \|\mathbf{y} - \mathbf{x}\|_2|. \quad (48)$$

Next, applying the Cauchy-Schwarz inequality on the right-hand side and identifying  $\|\mathbf{v}\|_2 = \|\mathbf{y} - \mathbf{x}\|_2$  yields

$$|L(\mathbf{y}) - L(\mathbf{x})| \leq \|\nabla L(\mathbf{x})\|_2 \cdot \|\mathbf{y} - \mathbf{x}\|_2 + \|\mathbf{u}\|_2 \cdot \|\mathbf{y} - \mathbf{x}\|_2^2. \quad (49)$$

The vector  $\mathbf{u}$  can be further reformulated as  $\mathbf{u} = \mathbf{L}_0 + \mathbf{L}_1 \odot |\nabla L(\mathbf{x})|$ , where  $\odot$  denotes the Hadamard product and  $\nabla L(\mathbf{x})$  is the gradient vector of  $L$ . This eventually yields the statement in Lemma 2.

## APPENDIX B PROOF OF PROPOSITION 2

Plugging in  $e_q, \hat{e}_q$  into the upper bound on the loss divergence in (12) and taking the gradient w.r.t.  $e_q$  ( $\nabla_{e_q}$ ) gives

$$|L(e_q) - L(\hat{e}_q)| \leq \|\nabla_{e_q} L(e_q)\|_2 \cdot \|e_q - \hat{e}_q\|_2 + \|\mathbf{L}_0 + \mathbf{L}_1 \odot |\nabla_{e_q} L(e_q)|\|_2 \cdot \|e_q - \hat{e}_q\|_2^2. \quad (50)$$

Further, substituting by  $\mathbf{u}(e_q)$  from (21) and taking the expectation over the joint distribution of  $\{s_{qnk}\}_{(n,k) \in \mathcal{R}_q}$  yields

$$\mathbb{E}[|L(e_q) - L(\hat{e}_q)|] \leq \mathbb{E}[\|\nabla_{e_q} L(e_q)\|_2 \cdot \|e_q - \hat{e}_q\|_2] + \mathbb{E}[\|\mathbf{u}(e_q)\|_2 \cdot \|e_q - \hat{e}_q\|_2^2]. \quad (51)$$

With non-negative expectations, the Cauchy-Schwarz inequality, i.e.  $\mathbb{E}[A \cdot B] \leq \sqrt{\mathbb{E}[A^2] \cdot \mathbb{E}[B^2]}$ , can be applied. Further, as  $\nabla_{e_q} L(e_q)$  and  $\mathbf{u}(e_q)$  are independent of  $s_{qnk}$  and with  $\mathbb{E}[\|e_q - \hat{e}_q\|_2^2] = \mathbb{E}[\|s_q - \hat{s}_q\|_2^2]$  from Proposition 1, we obtain the following statement of Proposition 2:

$$\mathbb{E}[|L(e_q) - L(\hat{e}_q)|] \leq \|\nabla_{e_q} L(e_q)\|_2 \cdot \sqrt{\mathbb{E}[\|s_q - \hat{s}_q\|_2^2]} + \|\mathbf{u}(e_q)\|_2 \cdot \mathbb{E}[\|s_q - \hat{s}_q\|_2^2]. \quad (52)$$

## REFERENCES

- [1] W. Saad, O. Hashash, C. K. Thomas, C. Chaccour, M. Debbah, N. Mandayam, and Z. Han, "Artificial General Intelligence (AGI)-Native Wireless Systems: A Journey Beyond 6G," *arXiv preprint arXiv:2405.02336*, 2024.
- [2] W. Saad, M. Bennis, and M. Chen, "A Vision of 6G Wireless Systems: Applications, Trends, Technologies, and Open Research Problems," *IEEE Network*, vol. 34, no. 3, pp. 134–142, 2019.
- [3] V. Ziegler, P. Schneider, H. Viswanathan, M. Montag, S. Kanugovi, and A. Rezaki, "Security and Trust in the 6G Era," *IEEE Access*, vol. 9, pp. 142 314–142 327, 2021.
- [4] M. Chen, D. Gündüz, K. Huang, W. Saad, M. Bennis, A. V. Feljan, and H. V. Poor, "Distributed Learning in Wireless Networks: Recent Progress and Future Challenges," *IEEE Journal on Selected Areas in Communications*, vol. 39, no. 12, pp. 3579–3605, 2021.
- [5] A. Yazdinejad, A. Dehghantanha, H. Karimpour, G. Srivastava, and R. M. Parizi, "A Robust Privacy-Preserving Federated Learning Model Against Model Poisoning Attacks," *IEEE Transactions on Information Forensics and Security*, pp. 1–1, 2024.
- [6] S. Qiu, Q. Liu, S. Zhou, and C. Wu, "Review of Artificial Intelligence Adversarial Attack and Defense Technologies," *Applied Sciences*, vol. 9, no. 5, p. 909, 2019.
- [7] B. D. Son, N. T. Hoa, T. Van Chien, W. Khalid, M. A. Ferrag, W. Choi, and M. Debbah, "Adversarial Attacks and Defenses in 6G Network-Assisted IoT Systems," *IEEE Internet of Things Journal*, 2024.
- [8] California State Legislature, "California Consumer Privacy Act of 2018," [https://leginfo.ca.gov/faces/codes\\_displayText.xhtml?division=3.&part=4.&lawCode=CIV&title=1.81.5](https://leginfo.ca.gov/faces/codes_displayText.xhtml?division=3.&part=4.&lawCode=CIV&title=1.81.5), 2018.
- [9] B. McMahan, E. Moore, D. Ramage, S. Hampson, and B. A. y Arcas, "Communication-Efficient Learning of Deep Networks from Decentralized Data," in *Artificial Intelligence and Statistics*. PMLR, 2017, pp. 1273–1282.
- [10] C. Thapa, P. C. M. Arachchige, S. Camtepe, and L. Sun, "SplitFed: When Federated Learning Meets Split Learning," in *Proceedings of the AAAI Conference on Artificial Intelligence*, vol. 36, no. 8, 2022, pp. 8485–8493.
- [11] X. Jiao, Y. Yin, L. Shang, X. Jiang, X. Chen, L. Li, F. Wang, and Q. Liu, "TinyBERT: Distilling BERT for Natural Language Understanding," *arXiv preprint arXiv:1909.10351*, 2019.
- [12] M. Chen, H. V. Poor, W. Saad, and S. Cui, "Wireless Communications for Collaborative Federated Learning," *IEEE Communications Magazine*, vol. 58, no. 12, pp. 48–54, 2020.
- [13] W. Yang, L. Li, Z. Zhang, X. Ren, X. Sun, and B. He, "Be Careful about Poisoned Word Embeddings: Exploring the Vulnerability of the Embedding Layers in NLP Models," *arXiv preprint arXiv:2103.15543*, 2021.
- [14] K. Yoo and N. Kwak, "Backdoor Attacks in Federated Learning by Rare Embeddings and Gradient Ensembling," *arXiv preprint arXiv:2204.14017*, 2022.
- [15] Y. Shi and Y. E. Sagduyu, "Jamming Attacks on Federated Learning in Wireless Networks," *arXiv preprint arXiv:2201.05172*, 2022.
- [16] R. Ruby, H. Yang, and K. Wu, "Anti-Jamming Strategy for Federated Learning in Internet of Medical Things: A Game Approach," *IEEE Journal of Biomedical and Health Informatics*, vol. 27, no. 2, 2023.
- [17] G. P. Fettweis and H. Boche, "On 6G and Trustworthiness," *Commun. ACM*, vol. 65, no. 4, p. 48–49, Mar 2022.
- [18] G. Marti, T. Kölle, and C. Studer, "Mitigating Smart Jammers in Multi-User MIMO," *IEEE Transactions on Signal Processing*, vol. 71, pp. 756–771, 2023, arXiv:2208.01453.
- [19] G. Marti and C. Studer, "Universal MIMO Jammer Mitigation via Secret Temporal Subspace Embeddings," May 2023, arXiv:2305.01260.
- [20] J. Gao, S. A. Vorobyov, H. Jiang, and H. V. Poor, "Worst-Case Jamming on MIMO Gaussian Channels," *IEEE Transactions on Signal Processing*, vol. 63, no. 21, pp. 5821–5836, 2015.
- [21] A. Kashyap, T. Basar, and R. Srikant, "Correlated Jamming on MIMO Gaussian Fading Channels," *IEEE Transactions on Information Theory*, vol. 50, no. 9, pp. 2119–2123, 2004.
- [22] V. C. Andrei, A. Djuhera, X. Li, U. J. Mönich, H. Boche, and W. Saad, "Resilient-By-Design Framework for MIMO-OFDM Communications under Smart Jamming," *IEEE International Conference on Communications*, 2024.
- [23] W. Yu, W. Rhee, S. Boyd, and J. M. Cioffi, "Iterative Water-Filling for Gaussian Vector Multiple-Access Channels," *IEEE Transactions on Information Theory*, vol. 50, no. 1, pp. 145–152, 2004.
- [24] N. Jain, P.-y. Chiang, Y. Wen, J. Kirchenbauer, H.-M. Chu, G. Somepalli, B. R. Bartoldson, B. Kailkhura, A. Schwarzschild, A. Saha *et al.*, "NEFTune: Noisy Embeddings Improve Instruction Finetuning," *arXiv preprint arXiv:2310.05914*, 2023.
- [25] J. Geiping, H. Bauermeister, H. Dröge, and M. Moeller, "Inverting Gradients – How Easy is it to Break Privacy in Federated Learning?" *Advances in neural information processing systems*, vol. 33, pp. 16937–16947, 2020.
- [26] Z. Chen, P. Chen, Z. Guo, Y. Zhang, and X. Wang, "A RIS-Based Vehicle DOA Estimation Method With Integrated Sensing and Communication System," *IEEE Transactions on Intelligent Transportation Systems*, vol. 25, no. 6, pp. 5554–5566, 2024.
- [27] P. Chen, Z. Yang, Z. Chen, and Z. Guo, "Reconfigurable Intelligent Surface Aided Sparse DOA Estimation Method With Non-ULA," *IEEE Signal Processing Letters*, vol. 28, pp. 2023–2027, 2021.
- [28] C. Chaccour, W. Saad, M. Debbah, and H. V. Poor, "Joint Sensing, Communication, and AI: A Trifecta for Resilient THz User Experiences," *IEEE Transactions on Wireless Communications*, 2024.
- [29] W. Wei, L. Liu, Y. Wut, G. Su, and A. Iyengar, "Gradient-Leakage Resilient Federated Learning," in *2021 IEEE 41st International Conference on Distributed Computing Systems (ICDCS)*. IEEE, 2021, pp. 797–807.
- [30] K. Bonawitz, V. Ivanov, B. Kreuter, A. Marcedone, H. B. McMahan, S. Patel, D. Ramage, A. Segal, and K. Seth, "Practical Secure Aggregation for Federated Learning on User-Held Data," *arXiv preprint arXiv:1611.04482*, 2016.
- [31] M. Chen, Z. Yang, W. Saad, C. Yin, H. V. Poor, and S. Cui, "A Joint Learning and Communications Framework for Federated Learning Over Wireless Networks," *IEEE Transactions on Wireless Communications*, vol. 20, no. 1, pp. 269–283, 2021.
- [32] M. Crawshaw, M. Liu, F. Orabona, W. Zhang, and Z. Zhuang, "Robustness to Unbounded Smoothness of Generalized SignSGD," in *Advances in Neural Information Processing Systems*, S. Koyejo, S. Mohamed, A. Agarwal, D. Belgrave, K. Cho, and A. Oh, Eds., vol. 35. Curran Associates, Inc., 2022, pp. 9955–9968.
- [33] J. Zhang, T. He, S. Sra, and A. Jadbabaie, "Why Gradient Clipping Accelerates Training: A Theoretical Justification for Adaptivity," *arXiv preprint arXiv:1905.11881*, 2019.
- [34] V. C. Andrei, X. Li, U. J. Mönich, and H. Boche, "Sensing-Assisted Receivers for Resilient-By-Design 6G MU-MIMO Uplink," in *2023 IEEE 3rd International Symposium on Joint Communications and Sensing*, 2023, pp. 1–6.
- [35] G. Scutari, D. P. Palomar, and S. Barbarossa, "The MIMO Iterative Waterfilling Algorithm," *IEEE Transactions on Signal Processing*, vol. 57, no. 5, pp. 1917–1935, 2009.
- [36] S. Boyd and L. Vandenberghe, *Convex Optimization*. Cambridge University Press, March 2004.
- [37] H. Wolkowicz, R. Saigal, and L. Vandenberghe, *Handbook of Semidefinite Programming: Theory, Algorithms, and Applications*. Springer Science & Business Media, 2012, vol. 27.
- [38] J. Devlin, M.-W. Chang, K. Lee, and K. Toutanova, "BERT: Pre-training of Deep Bidirectional Transformers for Language Understanding," *arXiv preprint arXiv:1810.04805*, 2018.
- [39] Y. Liu, M. Ott, N. Goyal, J. Du, M. Joshi, D. Chen, O. Levy, M. Lewis, L. Zettlemoyer, and V. Stoyanov, "RoBERTa: A Robustly Optimized BERT Pretraining Approach," *arXiv preprint arXiv:1907.11692*, 2019.
- [40] R. Socher, A. Perelygin, J. Wu, J. Chuang, C. D. Manning, A. Y. Ng, and C. Potts, "Recursive Deep Models for Semantic Compositionality Over a Sentiment Treebank," in *Proceedings of the 2013 Conference on Empirical Methods in Natural Language Processing*, 2013, pp. 1631–1642.
- [41] A. Wang, A. Singh, J. Michael, F. Hill, O. Levy, and S. R. Bowman, "GLUE: A Multi-Task Benchmark and Analysis Platform for Natural Language Understanding," *arXiv preprint arXiv:1804.07461*, 2018.
- [42] A. Williams, N. Nangia, and S. R. Bowman, "A Broad-Coverage Challenge Corpus for Sentence Understanding through Inference," *arXiv preprint arXiv:1704.05426*, 2017.
- [43] E. F. Sang and F. De Meulder, "Introduction to the CoNLL-2003 Shared Task: Language-Independent Named Entity Recognition," *arXiv preprint cs/0306050*, 2003.
- [44] L. Derczynski, E. Nichols, M. Van Erp, and N. Limsopatham, "Results of the WNUT2017 Shared Task on Novel and Emerging Entity Recognition," in *Proceedings of the 3rd Workshop on Noisy User-generated Text*, 2017, pp. 140–147.
- [45] A. Liu, X. Liu, H. Yu, C. Zhang, Q. Liu, and D. Tao, "Training Robust Deep Neural Networks via Adversarial Noise Propagation," *IEEE Transactions on Image Processing*, vol. 30, pp. 5769–5781, 2021.